

Kinetic versus Thermodynamic Control in the Deprotonation of Unsymmetrical Ketones in the Gas Phase

Leonard J. Chyall, Mark D. Brickhouse, Mark E. Schnute, and Robert R. Squires*

Contribution from the Department of Chemistry, Purdue University,
West Lafayette, Indiana 47907-1393

Received April 28, 1994*

Abstract: An experimental method is presented for determining the regioselectivity of deprotonation of unsymmetrical ketones in the gas phase. Mixtures of tautomeric enolate ions were prepared in a flowing afterglow apparatus and then assayed through a reaction with *n*-butyl nitrite in the collision cell of a triple quadrupole mass analyzer. Enolate ions were also prepared regioselectively by desilylation of the corresponding trimethylsilyl enol ethers with fluoride ion. Rate coefficients for the methanol-catalyzed tautomerization of the regioisomers were measured and were used to derive the equilibrium ratio of the tautomers. For 2-butanone it was found that the equilibrium mixture of enolate ions consisted of 55% of the more substituted isomer. For 3-methyl-2-butanone and 2-methyl-3-pentanone the equilibrium mixture comprised greater than 95% of the less substituted isomer. Several different bases were used to prepare nonequilibrium mixtures of enolate ions. Strong bases deprotonate these ketones irreversibly and in a statistical fashion. Deprotonation with hindered bases altered the composition of regioisomers only slightly. *Ab initio* molecular orbital calculations were performed on 2-butanone, 3-methyl-2-butanone, and their corresponding enolate ions at the MP4SDQ/6-31+G(d)//HF/6-31+G(d) level of theory. For 2-butanone, the calculations predict that the *Z* secondary enolate and the primary enolate have equal stabilities ($\Delta E < 0.1$ kcal/mol), while the *E* secondary enolate is 4.1 kcal/mol higher in energy than the *Z* enolate ion. For 3-methyl-2-butanone, the tertiary enolate ion is calculated to be 4.3 kcal/mol higher in energy than the primary enolate ion. The computed gas-phase acidities of the two ketones are in excellent agreement with the experimentally determined values.

Introduction

The regioselective deprotonation of an unsymmetrical ketone is critical to the success of many organic reactions. For example, the aldol condensation is a widely used reaction that often relies upon the availability of an enolate ion that is regiochemically and diastereomerically pure.¹ Accordingly, much effort has gone into understanding the factors that influence the site of deprotonation of an unsymmetrical ketone. A key consideration is whether deprotonation is carried out under "kinetic" or "thermodynamic" conditions. Kinetic conditions imply that proton transfer is rapid, quantitative, and irreversible, while equilibrium conditions imply that proton transfer is reversible such that the resulting mixture of enolate ions is indicative of the relative thermodynamic stability of each isomer. The original studies in this area, particularly those by House and co-workers, serve as textbook examples of these important concepts.^{2,3} From these and subsequent studies, it has become clear that the composition of tautomeric mixtures of enolate ions is due to a complex balance between the intrinsic stabilities of the isomers and several extrinsic factors. For example, it has been shown that the identity of the base and the corresponding counterion, the type of solvent used, the reaction temperature, and the degree of aggregation of the species involved can all have a significant influence on the regioselectivity of the deprotonation.

In recent reports from this laboratory, we have described several

aspects of the gas-phase properties and reactivity of enolate ions,⁴ including C vs O regioselectivity in alkylation reactions,⁵ gas-phase acidities and Bronsted vs Lewis acid-base reactivity with 6,6-dimethylfulvene,⁶ and unimolecular decomposition reactions.⁷ In this paper we describe an experimental method for determining the relative thermodynamic stabilities of unsolvated tautomeric enolate ions derived from unsymmetrical ketones as well as the gas-phase reactivity of several anionic bases toward unsymmetrical ketones. By examining this chemistry in the gas phase, it is possible to eliminate the influences of solvation, aggregation, and counterion pairing on the regioselectivity of enolate formation. Once the intrinsic (gas-phase) behavior is established, comparisons can be made to results obtained in solution so that the relative importance of the various extrinsic factors can be evaluated. This study encompasses the chemistry of the tautomeric enolate ions derived from three simple unsymmetrical ketones: 2-butanone (methyl ethyl ketone), 3-methyl-2-butanone (methyl isopropyl ketone), and 2-methyl-3-pentanone (ethyl isopropyl ketone).

The flowing afterglow-triple quadrupole technique is well-suited for kinetic and thermodynamic studies of enolate formation. These anions can be generated in a room-temperature bath of helium without counterions or solvent molecules, and their structures can be characterized using tandem mass spectrometry by examining either exothermic or endothermic reactions in the collision cell (Q2) of the triple quadrupole mass analyzer. We recently described experimental procedures for determining the kinetics of interconversion of isomeric or, more generally, isobaric ions (ions with the same mass-to-charge ratio) in the gas phase using monitor ion techniques.⁸ Herein, we describe the application of these methods to the analysis of mixtures of tautomeric enolate ions.

* Abstract published in *Advance ACS Abstracts*, September 1, 1994.
(1) (a) Mukaiyama, T. *Org. Reactions* **1982**, *28*, 203. (b) Evans, D. A. In *Asymmetric Synthesis*; Morrison, J. D., Ed.; Academic: New York, 1983; Vol. 3, Chapter 1. (c) Braun, M. In *Advances in Carbanion Chemistry*; Sniekus, V., Ed.; JAI Press: Greenwich, CT, 1992; Vol. 1, pp 177-247.
(2) (a) Carey, F. A.; Sundberg, R. J. *Advanced Organic Chemistry*, 3rd ed.; Plenum: New York, 1990; Part A, pp 407-414, Part B, pp 1-11. (b) Caine, D. In *Carbon-Carbon Bond Formation*; Augustine, R. L., Ed.; Plenum: New York, 1988; Chapter 2. (c) Heathcock, C. H. In *Modern Synthetic Methods*; Scheffold, R., Ed.; VCH: Weinheim, 1992. Chapter 1.
(3) (a) House, H. O. *Modern Synthetic Reactions*, 2nd ed; W. A. Benjamin: Menlo Park, CA, 1972. (b) House, H. O. *Rec. Chem. Prog.* **1967**, *28*, 99. (c) House, H. O.; Czuba, L. J.; Gall, M.; Olmstead, H. D. *J. Org. Chem.* **1969**, *34*, 2324.

(4) Squires, R. R. *Acc. Chem. Res.* **1992**, *25*, 461.
(5) Brickhouse, M. D.; Squires, R. R. *J. Phys. Org. Chem.* **1989**, *2*, 389.
(6) Brickhouse, M. D.; Squires, R. R. *J. Am. Chem. Soc.* **1988**, *110*, 2706.
(7) Graul, S. T.; Squires, R. R. *J. Am. Chem. Soc.* **1990**, *112*, 2517.
(8) Brickhouse, M. D.; Chyall, L. J.; Sunderlin, L. S.; Squires, R. R. *Rapid Commun. Mass Spectrom.* **1993**, *7*, 383.

Experimental Section

All experiments were performed at room temperature with a flowing afterglow triple-quadrupole instrument that has been previously described in detail.⁹ Enolate ions were generated in the helium flow reactor, which was maintained at a total pressure of 400 mTorr. The ions were extracted through an orifice into the low pressure chamber that houses the triple quadrupole mass analyzer. Mass selection was performed with the first quadrupole (Q1), and the ions of interest were then focused into the rf-only, gas-tight, second quadrupole (Q2), which contained 0.09–0.15 mTorr of the reagent gas. When examining exothermic ion/molecule reactions taking place in the triple quadrupole analyzer, the Q2 pole bias was kept low (0.8–1.0 V) to minimize the kinetic energy of the reactant ion. The product ions were then mass-analyzed with Q3, with the pole bias kept above 5 V (relative to Q2) to permit efficient extraction and transmission of the product ions. The ions were detected with an electron multiplier operating in pulse-counting mode under conditions that minimize mass-discrimination. Collision-induced dissociation (CID) of enolate ions was performed in Q2 with argon as the target gas under single-collision conditions ($P(\text{Ar}) < 0.05$ mTorr). The enolate ions of the ketones studied were produced by proton transfer to a variety of bases. Amide was produced by electron impact (EI) on anhydrous ammonia. Hydroxide was produced by EI on a 1:2 mixture of N_2O and CH_4 . Fluoride was generated by electron impact on nitrogen trifluoride. Diisopropylamide, tetramethylpiperide, cyanomethyl anion (CH_2CN^-) and 2-cyano-2-propyl anion ($(\text{CH}_3)_2\text{CCN}^-$) were produced by deprotonation of the corresponding parent acids with amide. Regioselective generation of the ketone enolate ions was performed by desilylation of the appropriate trimethylsilyl enol ethers with either fluoride or amide.

The trimethylsilyl enol ethers were synthesized using previously reported methods.^{3c,10} When necessary, the mixture of isomeric trimethylsilyl enol ethers was separated by preparative gas chromatography using a $12' \times 4$ mm column of 15% OV-101 (dimethylsilicone) liquid phase on 60/80 mesh Chromosorb W-NAW (HMDS). Subsequent 200 MHz ^1H NMR analysis of the separated trimethylsilyl enol ethers showed no detectable cross-contamination of the isomers. The ketones 2-butanone, 3-methyl-2-butanone, and 2-methyl-3-pentanone were distilled from phosphorus pentoxide prior to use. Diisopropylamine, tetramethylpiperidine, acetonitrile, and isobutyronitrile were distilled from calcium hydride prior to use. *n*-Butyl nitrite was washed several times with water and aqueous sodium bicarbonate, dried over anhydrous magnesium sulfate, and distilled *in vacuo* prior to use. Methanol was distilled from magnesium methoxide prior to use. All samples were subjected to several freeze-pump-thaw cycles in order to remove dissolved gases. Gas purities were as follows: He (99.995%), CH_4 (99.0%), N_2O (99.0%), NF_3 (99.0%), and NH_3 (anhydrous, 99.5%).

Ab initio molecular orbital calculations were performed on an IBM RISC/6000 computer using the Gaussian 92 series of programs.¹¹ Geometries were optimized employing C_1 or C_s symmetry with a 6-31+G(d) basis set¹² and were determined to correspond to true minima by the absence of negative eigenvalues in the matrix of computed force constants. The calculated frequencies were scaled by a factor of 0.89 for all zero-point energy corrections. Single-point energies were obtained using fourth-order Møller–Plesset perturbation theory (frozen-core), including all single-, double-, and quadruple-excitations, *i.e.*, MP4SDQ/6-31+G(d)//HF/6-31+G(d). For the 2-butanone system, the effects of triple excitations were also evaluated with single-point energy calculations at the MP4SDTQ/6-31+G(d) level. The minor differences in heat capacities were ignored in the calculations of the relative energies and proton affinities.

Results

What is to follow is a description of how ketones are deprotonated in the gas phase under “kinetic” and “thermo-

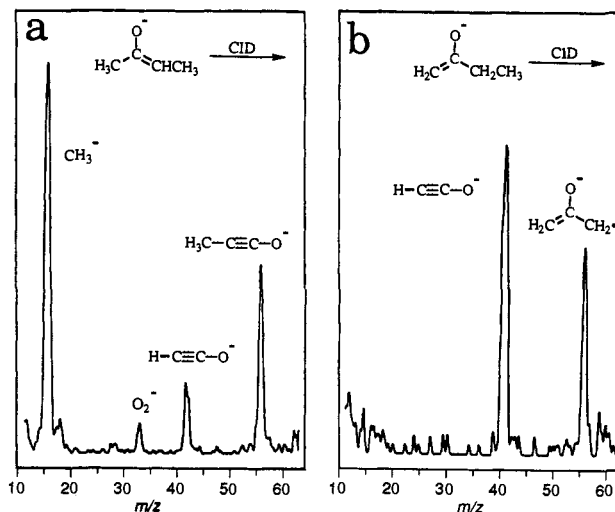


Figure 1. Product mass spectra obtained from collision-induced dissociation of the (a) primary and (b) secondary enolate ions of 2-butanone.

dynamic” conditions. It will be shown that the resulting enolate ions can be qualitatively distinguished by observing distinct product ions produced upon collision-induced dissociation and through an exothermic ion–molecule reaction with *n*-butyl nitrite. The latter process is used to determine the ratio of tautomeric enolate ions that are present in the flow tube of the instrument. Acid-catalyzed tautomerization of the enolate ions with methanol added to the flow-tube permits determination of the equilibrium ratios of enolate ions, while irreversible deprotonation of the ketones with various bases is used to determine the enolate ion compositions that are produced under “kinetic” conditions.

Collision-Induced Dissociation of the Enolate Ions of 2-Butanone. In principle, the site of deprotonation of an unsymmetrical, unlabeled ketone in the gas phase can be determined by collision-induced dissociation (CID) of the corresponding enolate ion. Detailed studies of various enolate ions have shown that several structure-dependent dissociations are operative.¹³ However, experiments performed with deuterium-labeled compounds have shown that enolate ion fragmentation mechanisms can be quite complex and that the observed product ions are often produced by several fragmentation pathways.^{13,14} Nonetheless, it was of interest to examine whether enolate ion CID could be used as a quantitative tool for assaying the composition of an unknown mixture of regioisomers produced in the flowing afterglow apparatus.

The enolate ions of 2-butanone were formed regioselectively by either amide-induced or fluoride-induced desilylation of the corresponding trimethylsilyl enol ethers. The regioselectivity of these reactions has been previously demonstrated.¹⁵ Shown in Figure 1 are the product ion spectra resulting from low energy (22 eV lab) CID of the primary enolate ion (1) and secondary enolate ion (2) of 2-butanone with argon target gas. The primary enolate ion dissociates to produce ions of m/z 41 and m/z 56, which are even-electron and odd-electron species, respectively. The ion of m/z 41 is assigned to the ketylenyl anion, which is believed to form by loss of ethane *via* a two-step mechanism.^{16,17} The ion of m/z 56 is formed by homolytic cleavage of a methyl group to give the oxyallyl radical anion (Scheme 1). Similar processes

(13) (a) Bowie, J. H. *Mass Spectrom. Rev.* **1984**, *3*, 161. (b) Bowie, J. H. *Mass Spectrom. Rev.* **1990**, *9*, 349.

(14) (a) Stringer, M. B.; Bowie, J. H.; Holmes, J. L. *J. Am. Chem. Soc.* **1986**, *108*, 3888. (b) Bowie, J. H.; Stringer, M. B.; Currie, G. J. *J. Chem. Soc., Perkin Trans. II* **1986**, 1821. (c) Currie, G. J.; Stringer, M. B.; Bowie, J. H.; Holmes, J. L. *Aust. J. Chem.* **1987**, *40*, 1365.

(15) Squires, R. R.; DePuy, C. H. *Org. Mass Spectrom.* **1982**, *17*, 187.

(16) (a) Donnelly, A.; Chowdhury, S. K.; Harrison, A. G. *Org. Mass Spectrom.* **1989**, *24*, 89. (b) Chowdhury, S. K.; Harrison, A. G. *Org. Mass Spectrom.* **1990**, *25*, 637. (c) Chowdhury, S. K.; Harrison, A. G. *Int. J. Mass Spectrom. Ion Processes* **1989**, *92*, 135.

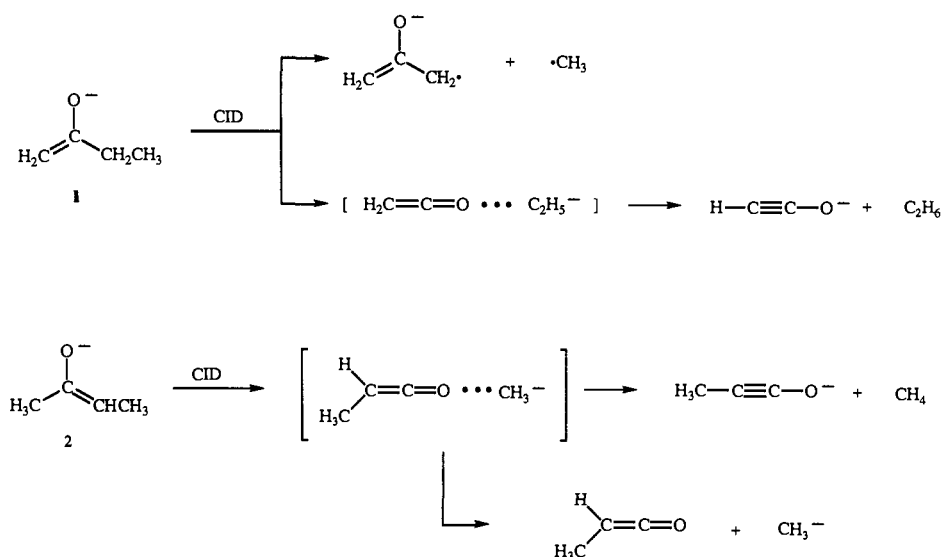
(9) (a) Marinelli, P. J.; Paulino, J. A.; Sunderlin, L. S.; Wenthold, P. G.; Poutsma, J. C.; Squires, R. R. *Int. J. Mass Spectrom. Ion Processes* **1994**, *130*, 89. (b) Graul, S. T.; Squires, R. R. *Mass Spectrom. Rev.* **1988**, *7*, 263.

(10) (a) Rubottom, G. M.; Mott, R. C.; Krueger, D. S. *Synth. Commun.* **1977**, *7*, 327. (b) Brown, C. A. *J. Org. Chem.* **1974**, *26*, 3913.

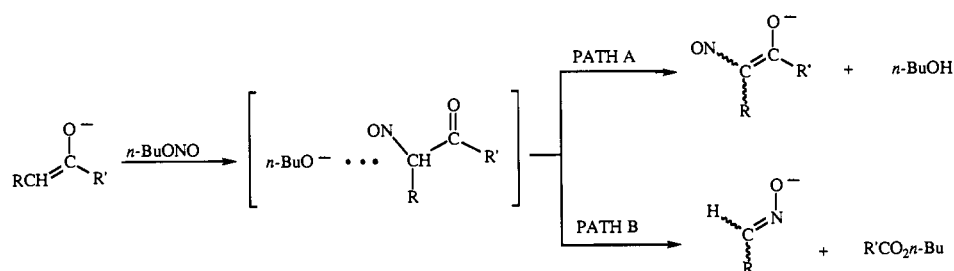
(11) Gaussian 92, Revision D.2; Frisch, M. J.; Trucks, G. W.; Head-Gordon, M.; Gill, P. M. W.; Wong, M. W.; Foresman, J. B.; Johnson, B. G.; Schlegel, H. B.; Robb, M. A.; Replogle, E. S.; Gomperts, R.; Andres, J. L.; Raghavachari, K.; Binkley, J. S.; Gonzalez, C.; Martin, R. L.; Fox, D. J.; Defrees, D. J.; Baker, J.; Stewart, J. P.; Pople, J. A. Gaussian, Inc.: Pittsburgh, PA, 1992.

(12) Hariharan, P. C.; Pople, J. A. *Theor. Chim. Acta* **1973**, *28*, 213. (b) Spitznagel, G. W.; Clark, T.; Chandrasekhar, J.; Schleyer, P. v. R. *J. Comput. Chem.* **1982**, *3*, 363. (c) Clark, T.; Chandrasekhar, J.; Spitznagel, G. W.; Schleyer, P. v. R. *J. Comput. Chem.* **1983**, *4*, 294.

Scheme 1



Scheme 2



have also been observed for other enolate ions such as that derived from 2-pentanone.^{16a} The secondary enolate ion of 2-butanone produces CID product ions that are different from those derived from the primary enolate ion. The major product ion of m/z 15 is the methyl anion, and the ions of m/z 41 and m/z 55 are assigned to the ketenyl anion and the methylketenyl anion, respectively (Scheme 1). While the methylketenyl anion is believed to be formed by an analogous pathway as that shown for the formation of the ketenyl anion from the primary enolate ion, the mechanism for the formation of the ketenyl anion from the secondary enolate ion is unclear. One possibility is for the secondary enolate ion of 2-butanone to rearrange to the primary enolate ion prior to dissociation.¹⁸

The unique product ions observed upon collisional activation of the tautomeric enolate ions permit the differentiation of these isomers. Ideally, analysis of the ratios of the unique product ions could permit the quantitative determination of mixtures of enolate ions. However, certain practical limitations render this method unsuitable for the present study. The extent of collision-induced electron detachment, which could differ for the two enolate isomers and for the CID product ions, cannot be determined reliably. Therefore, the observed ratio of fragment ions signal intensities may not accurately reflect the relative abundances of the isomeric parent ions in the mixture. Moreover, it was observed that the relative abundances of the fragment ions are strongly dependent on the collision energy, which leads to poor reproducibility in the measurement of product ion ratios, and increases the overall error associated with the analysis. For these reasons, an alternate method for the quantitative determination of enolate ions was devised.

Quantitation of Enolate Ions. Exothermic reactions between enolate ions and certain reagent gases in Q2 can provide a more practical method for determining the relative concentrations of isomers. We have found that alkyl nitrites are ideal reagents for the differentiation and quantitation of tautomeric enolate ions.

Several earlier investigations have demonstrated that alkyl nitrites undergo a variety of reactions with gas-phase anions that can be useful as probes of their structure.¹⁹ In particular, alkyl nitrites react with tautomeric enolate ions to yield structurally diagnostic product ions.¹⁵ Illustrated in Scheme 2 are the two most important product channels for the reaction of *n*-butyl nitrite with an enolate ion. These product ions are formed by initial nitrosation of the enolate ion to give an intermediate complex consisting of butoxide ion and an α -nitrosoketone. The butoxide ion can deprotonate the α -nitrosoketone to yield a nitrosated enolate as the ionic product (Scheme 2, path A). The intermediate complex can also dissociate (presumably by a retro-Claisen reaction) to yield an α -nitrosocarbanion as the ionic product (Scheme 2, path B). Other ionic products are also generated, in typical yields less than 20%, when enolate ions are allowed to react with *n*-butyl nitrite (Table 1). Carboxylate ions and ketenyl ions are observed in varying amounts depending upon the structure of the enolate ion. An elimination reaction most likely accounts for the formation of NO_2^- . The mechanistic details of these reactions have been described previously.^{15,19}

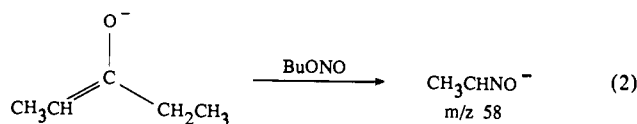
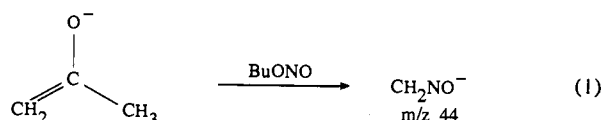
As shown in path B of Scheme 2, α -nitrosocarbanions are produced in the reaction of enolate ions with *n*-butyl nitrite. In this reaction, the alkyl group that is attached to the deprotonated carbon of the enolate ion is incorporated into the α -nitrosocarbanion product. For example, acetone enolate reacts with

(17) (a) Moylan, C. R.; Jasinski, J. M.; Brauman, J. I. *Chem. Phys. Lett.* **1983**, *98*, 1. (b) Foster, R. F.; Tumas, W.; Brauman, J. I. *J. Chem. Phys.* **1983**, *79*, 4644. (c) Moylan, C. R.; Jasinski, J. M.; Brauman, J. I. *J. Am. Chem. Soc.* **1985**, *107*, 1934.

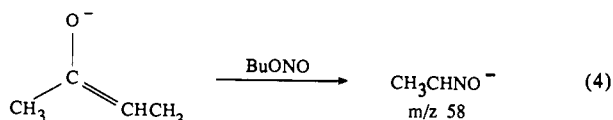
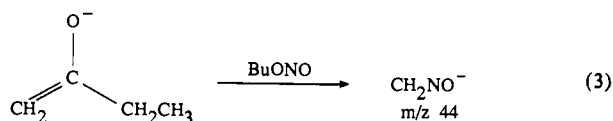
(18) It has been shown that certain enolate ions may tautomerize prior to dissociation: Hayes, R. N.; Sheldon, J. C.; Bowie, J. H. *Int. J. Mass Spectrom. Ion Processes* **1986**, *71*, 233.

(19) (a) Klass, G.; Bowie, J. H. *Aust. J. Chem.* **1980**, *33*, 2271. (b) Noest, A. J.; Nibbering, N. M. M. *Adv. Mass Spectrom.* **1980**, *8*, 227. (c) Noest, A. J.; Nibbering, N. M. M. *Int. J. Mass Spectrom. Ion Physics* **1980**, *34*, 383. (d) King, G. K.; Maricq, M. M.; Bierbaum, V. M.; DePuy, C. H. *J. Am. Chem. Soc.* **1981**, *103*, 7133.

n-butyl nitrite to give CH_2NO^- (m/z 44, eq 1), while 3-pentanone enolate reacts with *n*-butyl nitrite to give CH_3CHNO^- (m/z 58, equation 2).



This characteristic reactivity of *n*-butyl nitrite is suitable for identifying the site of deprotonation in an unsymmetrical ketone. Thus, the primary enolate ion of 2-butanone will react with *n*-butyl nitrite to give CH_2NO^- (eq 3), while the secondary enolate ion will give CH_3CHNO^- (eq 4).



Moreover, when a mixture of primary and secondary enolates is present, the measured yields of the two α -nitrosocarbanions will be proportional to the relative amounts of tautomeric enolates in the mixture.

The experimental strategy for quantitating mixtures of tautomeric enolate ions is as follows. Using pure enolate isomers obtained by fluoride-induced desilylation of the corresponding trimethylsilyl enol ethers, we must first determine the *absolute partial cross sections* for formation of the particular α -nitrosocarbanion that is to serve as the characteristic surrogate ion for the enolate isomer. The partial cross section for a reaction (σ_p) is given by the relative yield or *branching ratio* of the product of interest, multiplied by the total reaction cross section (eq 5). The total reaction cross section (σ_{tot}) is given by eq 6, where I_0 is the reactant

$$\sigma_p = [I_p / \sum I_p] \sigma_{\text{tot}} \quad (5)$$

$$\sigma_{\text{tot}} = -\ln [I_0 / (I_0 + \sum I_p)] / nL \quad (6)$$

ion intensity, I_p is the intensity of the individual product ions, n is the number density of *n*-butyl nitrite in Q2, and L is the effective ion path length for the reaction region.²⁰ Therefore, a plot of $-\ln [I_0 / (I_0 + \sum I_p)]$ vs $1/nL$ gives a straight line with a slope equal to σ_{tot} . The partial cross sections determined in the manner described above are then used to scale the measured nitrosocarbanion intensity ratios obtained from a mixture of tautomeric enolate ions, thereby accounting for the inherent difference in reactivity between the two enolate ions toward the *n*-butyl nitrite probe reagent. In this way, the scaled ratio of nitrosocarbanion surrogate ions produced upon reaction with *n*-butyl nitrite in Q2

(20) The physical length of Q2 is 20 cm, but the true path length of the ions is slightly larger due to oscillatory motion of ions inside a quadrupole field, and because small quantities of reagent gas are present outside of the reaction chamber. The effective path length of the reaction region was found to be 24 cm by calibration against the reaction $\text{Ar}^+ + \text{D}_2 \rightarrow \text{ArD}^+ + \text{D}$. See: Ervin, K. M.; Armentrout, P. B. *J. Chem. Phys.* **1985**, *83*, 166.

Table 1. Cross Sections and Product Ion Distributions for the Reaction of Various Enolate Ions with *n*-Butyl Nitrite

enolate ion	total cross section (\AA^2)	products	relative abundance	partial cross section (\AA^2)
$\begin{array}{c} \text{O}^- \\ \\ \text{H}_2\text{C}=\text{C}-\text{CH}_2\text{CH}_3 \\ \\ \text{CH}_3 \end{array}$	24	NO_2^-	0.10	2.4
		CH_2NO^-	0.19	4.6
		$\text{CH}_3\text{CH}_2\text{C}(\text{O})\text{CHNO}^-$	0.71	17.0
$\begin{array}{c} \text{O}^- \\ \\ \text{H}_3\text{C}-\text{C}=\text{CH}-\text{CH}_3 \\ \\ \text{CH}_3 \end{array}$	47	NO_2^-	0.19	8.9
		CH_3CHNO^-	0.41	19.3
		HCCO^-	0.01	0.5
		CH_3CO_2^-	0.10	4.7
		$\text{CH}_3\text{C}(\text{O})\text{C}(\text{CH}_3)\text{NO}^-$	0.29	13.6
$\begin{array}{c} \text{O}^- \\ \\ \text{H}_2\text{C}=\text{C}-\text{CH}(\text{CH}_3)_2 \\ \\ \text{CH}_3 \end{array}$	14	NO_2^-	0.02	0.3
		CH_2NO^-	0.22	3.1
		$(\text{CH}_3)_2\text{CHC}(\text{O})\text{CHNO}^-$	0.76	10.6
$\begin{array}{c} \text{O}^- \\ \\ \text{H}_3\text{C}-\text{C}=\text{C}(\text{CH}_3)_2 \\ \\ \text{CH}_3 \end{array}$	59	NO_2^-	0.08	4.7
		$(\text{CH}_3)_2\text{CNO}^-$	0.58	34.2
		HCCO^-	0.17	10.0
		CH_3CO_2^-	0.14	8.3
		$(\text{CH}_3)_2(\text{NO})\text{CC}(\text{O})\text{CH}_2^-$	0.02	1.2
		$(\text{CH}_3)_2\text{CNO}^-$ (<i>n</i> -BuOH)	0.01	0.6
$\begin{array}{c} \text{O}^- \\ \\ \text{CH}_3\text{CH}=\text{C}-\text{CH}(\text{CH}_3)_2 \\ \\ \text{CH}_3 \end{array}$	59	NO_2^-	0.03	1.7
		CH_3CHNO^-	0.43	25.4
		$(\text{CH}_3)_2\text{CHC}(\text{O})\text{C}(\text{CH}_3)\text{NO}^-$	0.54	31.9
$\begin{array}{c} \text{O}^- \\ \\ \text{CH}_3\text{CH}_2-\text{C}=\text{C}(\text{CH}_3)_2 \\ \\ \text{CH}_3 \end{array}$	56	NO_2^-	0.05	2.8
		$(\text{CH}_3)_2\text{CNO}^-$	0.80	44.8
		CH_3CCO^-	0.09	5.0
		$\text{CH}_3\text{CH}_2\text{CO}_2^-$	0.01	0.6
		$(\text{CH}_3)_2(\text{NO})\text{CC}(\text{O})\text{CH}(\text{CH}_3)^-$	0.04	2.2
$(\text{CH}_3)_2\text{CNO}^-$ (<i>n</i> -BuOH)	0.01	0.6		

provides a direct measure of the ratio of tautomeric enolate ions present in the flow tube.

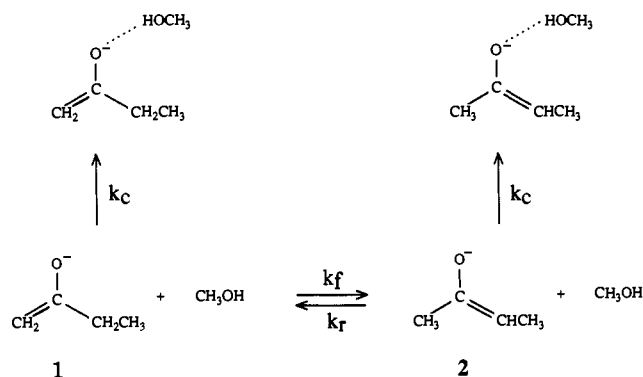
Table 1 provides a summary listing of the measured product ion branching ratios and total reaction cross sections for six different enolate ions, determined from experiments with each pure isomer. The relative yields of the product ions from each enolate were found to be constant over a wide range of *n*-butyl nitrite pressures, provided that a consistent set of ion lensing and extraction conditions were employed. It is evident that the total reaction cross sections as well as the partial cross sections for the nitrosocarbanion product channel can vary considerably for different pairs of tautomeric enolates. For comparison, the total reaction cross sections for reaction of these enolate ions with *n*-butyl nitrite calculated from trajectory-parameterized ion/molecule collision theory²¹ are on the order of 500 \AA^2 .

We illustrate the use of these data in assaying the mixture of enolate ions produced in the reaction between hydroxide ion and 2-butanone. When 2-butanone is deprotonated with hydroxide in the flow tube and the resulting mass-selected enolate ions are allowed to react with *n*-butyl nitrite in Q2, the observed ratio of intensities of the secondary enolate product (CH_3CHNO^-) and the primary enolate product (CH_2NO^-) is 3.5:1. From Table 1, it is apparent that the partial cross section for formation of CH_3CHNO^- is a factor of 4.2 greater than the partial cross section for formation of CH_2NO^- from the primary enolate. Therefore, the corrected ratio of secondary-to-primary enolate ions in the mixture is 3.5/4.2 or 0.83, *i.e.*, hydroxide ion deprotonates 2-butanone to give 55% of the *less-substituted* isomer.

Error in the above analysis results from the uncertainty associated with measuring the ratio of surrogate ion intensities and the uncertainty associated with measuring the absolute reaction cross sections. The reproducibility in measuring the relative intensities of the surrogate ions was typically better than 10%. The uncertainty associated with the total reaction cross sections is more difficult to evaluate. In particular, there may

(21) Su, T.; Chesnavich, W. J. *J. Chem. Phys.* **1982**, *76*, 5183.

Scheme 3



be a systematic error in the cross sections given in Table 1 due to the ill-defined length of the reaction region. However, this error will be the same for all of the measurements such that the relative error in the cross sections should be less than the absolute error. With these considerations in mind, error limits of $\pm 25\%$ are assigned to the measured ratios of surrogate ions.

Equilibration of Tautomeric Enolate Ions with Methanol. Isomerically pure enolate ions can be partially equilibrated by adding methanol downstream in the flow reactor. Methanol acts as an acid catalyst for this process, presumably by a series of proton transfer reactions within the ion-molecule collision complex. Competing with isomerization is the irreversible clustering between methanol and the enolate by termolecular association.²² In principle, a gas-phase enolate ion that is isomerically pure will eventually form an equilibrium mixture of tautomers given sufficient collisions with methanol molecules. The extent of isomerization can be monitored by comparing the relative intensities of the surrogate ions produced by reaction of the enolate mixture with *n*-butyl nitrite in Q2. Attainment of equilibrium would be indicated by a constant ratio of surrogate ion intensities with increasing methanol flow. In practice, equilibrium of the regiochemically pure enolate ions of 2-butanone was never achieved because of extensive attenuation of the signal due to irreversible clustering of the enolate ion with the added methanol.

An indirect method was designed to determine the equilibrium ratio of the tautomeric enolate ions of 2-butanone. The relevant kinetic scheme is illustrated in Scheme 3, where k_f and k_r are the rate coefficients for methanol-catalyzed isomerization of primary enolate (1) to secondary enolate (2) and the reverse reaction, respectively. The apparent bimolecular reaction rate coefficient for clustering of either enolate ion with methanol is given by k_c .²³ When 2-butanone enolates are generated in the flow tube and methanol is added, the observed change in signal intensities for the two surrogate ions formed in Q2 (CH_3CHNO^- from 2, and CH_2NO^- from 1) is due to two competing reactions: reversible methanol-catalyzed enolate isomer tautomerization and irreversible clustering. The appropriate differential equations derived from the kinetic scheme shown in Scheme 3 are given in eqs 7 and 8, where $d[1]/d[\text{CH}_3\text{OH}]$ and $d[2]/d[\text{CH}_3\text{OH}]$ represent

$$d[1]/d[\text{CH}_3\text{OH}] = -k_f t[1] + k_r t[2] - k_c t[1] \quad (7)$$

$$d[2]/d[\text{CH}_3\text{OH}] = -k_r t[2] + k_f t[1] - k_c t[2] \quad (8)$$

the rate of change of the surrogate ion signal intensities with

(22) (a) Caldwell, G.; Rozeboom, M. D.; Kiplinger, J. P.; Bartmess, J. E. *J. Am. Chem. Soc.* **1984**, *106*, 4660. (b) Meot-Ner, M.; Sieck, L. W. *J. Am. Chem. Soc.* **1986**, *108*, 7525.

(23) This kinetic model implicitly assumes that the two isomeric enolates undergo clustering with methanol with identical rate coefficients. Given the close similarities in the structures and charge distributions of the enolate isomers plus the essentially equal well-depths expected for interaction of either enolate with methanol, any differences in the clustering rate coefficients are likely to be negligibly small.

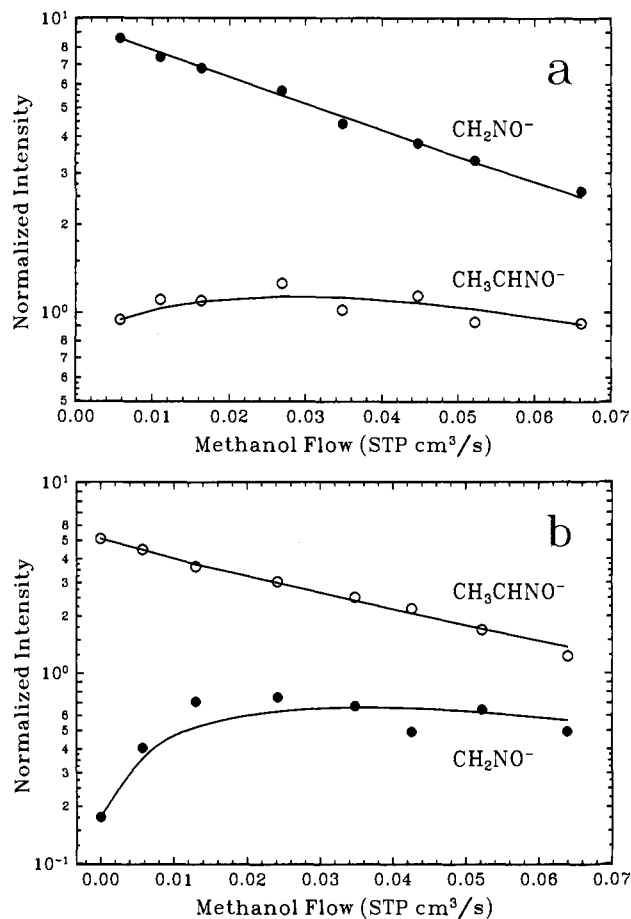


Figure 2. Surrogate ion intensity vs flow rate of added methanol during the partial equilibration of the (a) primary and (b) secondary enolate ions of 2-butanone.

changes in methanol flow rate, and t is the fixed time interval for reaction derived from the reaction distance in the flow tube (40 cm) and the bulk flow velocity (9400 cm/s). It follows that if the forward (k_f) and reverse (k_r) reaction rate coefficients for tautomerization and the rate coefficient for methanol clustering (k_c) are known, then the equilibrium constant, $K = (k_f/k_r)$, for the tautomeric pair of enolate ions may be determined.

The apparent bimolecular reaction rate coefficient for the clustering of methanol (k_c) with the enolate ions of 2-butanone was directly measured by monitoring the decrease in enolate ion intensity as a function of methanol flow rate. From 12 separate measurements this rate coefficient was found to be $k_c = 1.1 \pm 0.4 \times 10^{-10} \text{ cm}^3/\text{s}$. Direct measurement of k_f and k_r is not possible. However, these values can be determined by simulation of the experimental data with the kinetic model described above. In order to do this, the enolate ions of 2-butanone were prepared regioselectively by fluoride-induced desilylation of the corresponding trimethylsilyl enol ethers and then partially equilibrated with methanol. The extent of equilibration was measured as a function of added methanol by monitoring the change in intensity of the two surrogate α -nitrosocarbanions that were produced upon reaction of the mixture of enolate ions with *n*-butyl nitrite in Q2. The resulting data are shown in Figure 2, starting with nearly pure primary enolate (1) (Figure 2a) and nearly pure secondary enolate (2) (Figure 2b). The solid lines represent the optimal fit of each independent data set to the kinetic model outlined in Scheme 3, derived by numerical integration of the rate eqs 7 and 8 and simplex optimization of the values for k_f and k_r .²⁴ The rate coefficients derived from the data shown in Figure 2 (parts a and b) are listed in Table 2. In some of the simulations

Table 2. Derived Rate Coefficients (cm^3/s) for Methanol-Catalyzed Tautomerization of 2-Butanone Enolate Ions^a

enolate	k_f	k_r	k_c	K
1	3.5×10^{-11}	4.0×10^{-11}	1.2×10^{-10}	0.88
2	9.5×10^{-11}	5.7×10^{-11}	1.1×10^{-10}	1.67

^a Determined from simulation of the experimental data with the kinetic model shown in eq 7 and 8 starting with the indicated enolate isomer.

the clustering rate coefficient k_c was also allowed to vary independently. However, as indicated in Table 2, the optimized values for k_c turned out to be the same as the values directly measured. The values for k_f and k_r derived from the two independent simulations are in reasonable agreement, considering the nature of the measurement and the typical 25% uncertainty in flowing afterglow kinetics measurements. The average value of the equilibrium constant for 2-butanone enolate tautomerization is 1.27, corresponding to 56% of the secondary enolate 2.

It was found that complete equilibration of the enolate ions could only be achieved by preparing a mixture of enolate ions that is already close to the equilibrium ratio and then adding methanol to the flow tube. Deprotonation of 2-butanone with fluoride gives a mixture of tautomeric enolate ions that is near to the extrapolated equilibrium ratio calculated from the kinetic simulations. Addition of relatively low concentrations of methanol to the flow tube established equilibrium, as indicated by a constant ratio of surrogate ion signals with further addition of methanol. The equilibrium constant obtained in this manner (1.13) is in good agreement with the average value obtained from the simulations. Because of the greater number of sources of error associated with the kinetic method of determining the enolate equilibrium ratios, we used the direct method with fluoride as the primary base and methanol as the acid catalyst to determine the equilibrium ratios for the enolate ions derived from 3-methyl-2-butanone and 2-methyl-3-pentanone. The measured equilibrium ratios for the three enolate isomer pairs are listed in Table 3.

Computational Studies. The relative stabilities of the enolate ions derived from 2-butanone and 3-methyl-2-butanone were investigated using molecular orbital theory. *Ab initio* calculations of the structure and energy of 2-butanone have been performed previously.²⁵ Optimized geometries, zero-point vibrational energies, and correlation-corrected total energies were determined for the lowest energy conformers of 2-butanone, its primary enolate, and the *E* and *Z* diastereomeric secondary enolates as well as for 3-methyl-2-butanone and the corresponding primary and tertiary enolates. The total energies are listed in Table 4 and the geometries are partially summarized in Figure 3. Complete structural data and vibrational frequencies are available as supplementary material.²⁶ The (carbon) proton affinities and relative energies of the enolate ions were calculated using the total energies obtained at the MP4SDQ/6-31+G(d)//HF/6-31+G(d) level and zero-point energies derived from the scaled vibrational frequencies computed at the HF/6-31+G(d) level (Table 5). Additional single-point energy calculations that include triple excitations, *i.e.*, MP4SDTQ/6-31+G(d), were carried out for 2-butanone and the corresponding enolates. For the 2-butanone system, all levels of theory employed in this study predict that the primary enolate ion and the *Z* diastereomer of the secondary enolate are essentially identical in energy. The *E* diastereomer is predicted to be about 4 kcal/mol higher in energy than the other two enolates. The proton affinities of the two lower energy enolate ions calculated at the MP4SDTQ/6-31+G(d) level (367.7 kcal/mol) are in excellent agreement with the

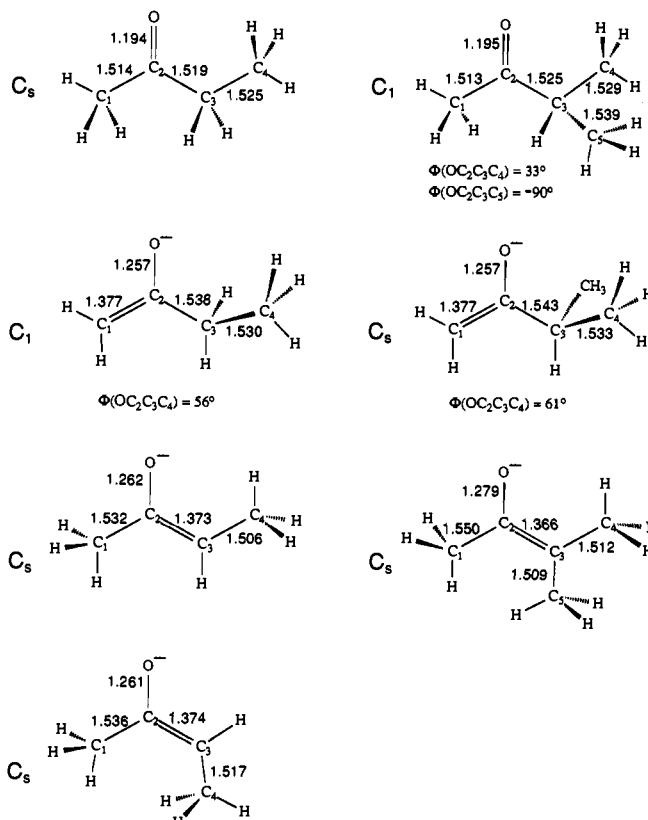


Figure 3. Optimized geometries for 2-butanone, 3-methyl-2-butanone, and associated enolates.

experimental gas-phase acidity of 368.1 ± 2.9 kcal/mol determined for 2-butanone by high-pressure mass spectrometry.^{27,28} For the 3-methyl-2-butanone system, theory predicts that the primary enolate is more stable than the tertiary enolate by 4.3 kcal/mol and that the gas-phase acidities of the α -methyl and isopropyl positions in 3-methyl-2-butanone are 369.5 and 373.8 kcal/mol, respectively. From the difference in calculated proton affinities of the 2-butanone enolates at the MP4SDQ and MP4SDTQ levels of theory, it is apparent that the inclusion of triple-excitations decreases the predicted proton affinities by 2.7 kcal/mol. Assuming an identical correction factor for the 3-methyl-2-butanone system, the corrected proton affinities for the primary and tertiary enolates are 366.8 and 371.1 kcal/mol, respectively. The former value is in excellent agreement with the experimentally determined gas-phase acidity of 3-methyl-2-butanone of 366.9 ± 2.9 kcal/mol.^{27,28}

Regioselectivity of Ketone Deprotonation with Various Bases.

The monitor ion technique can also be used to assay the nonequilibrium mixtures of tautomeric enolate ions that are produced when different bases are allowed to react with unsymmetrical ketones. In order for these results to be meaningful it must be known whether proton transfer can occur reversibly in the gas-phase ion-molecule collision complex, *i.e.*, whether partial equilibration of the enolate isomers can occur during the initial ion-molecule encounter by multiple proton exchanges between the ketone and the anionic base. One method for testing whether reversible proton transfer occurs within an ion-molecule collision complex is to use a deuterium-labeled anionic base that can transfer deuterium to the deprotonated substrate prior to the formation of separated products.²⁹ For example, if deprotonation

(27) Cumming, J. B.; Kebarle, P. *Can. J. Chem.* **1978**, *56*, 1.

(24) Suarez, R. L. MS Dissertation, Purdue University, 1990. The computer program is a modification of an earlier FORTRAN program written by K. L. Johnson and D. L. Doerfler at the University of Pittsburgh.

(25) (a) Wiberg, K. B.; Martin, E. *J. Am. Chem. Soc.* **1985**, *107*, 5035. (b) Wiberg, K. B.; Murko, M. A. *J. Comput. Chem.* **1988**, *9*, 488.

(26) Ordering information available on any current masthead page.

(28) Lias, S. G.; Bartmess, J. E.; Liebman, J. F.; Holmes, J. L.; Levin, R. D.; Mallard, W. G. *J. Phys. Chem. Ref. Data* **1988**, *17*, Suppl. 1. All data taken from the NIST Negative Ion Energetics Database, Version 3.00, NIST Standard Reference Database 19B, October 1993.

(29) Grabowski, J. J.; DePuy, C. H.; Bierbaum, V. M. *J. Am. Chem. Soc.* **1983**, *105*, 2565.

Table 3. Equilibrium Constants for Tautomeric Ketone Enolate Ions^a

ketone	more-substituted enolate ion (%)	less-substituted enolate ion (%)	equilibrium constant (<i>K</i>)
2-butanone	53	47	1.13
3-methyl-2-butanone	2	98	0.02
2-methyl-3-pentanone	5	95	0.05

^a Determined by methanol-catalyzed equilibration of the enolate mixture obtained by deprotonation of each ketone with fluoride ion.

of 2-butanone with OH⁻ is reversible within the ion-molecule collision complex, then deprotonation with OD⁻ would lead to the incorporation of deuterium into the enolate giving product ion signals for C₄H₇O⁻ (*m/z* 71) and C₄H₆DO⁻ (*m/z* 72). However, when isotopically pure OD⁻ was allowed to react with 2-butanone in a selected ion flow tube (SIFT) apparatus³⁰ only the M-H enolate ion with *m/z* 71 was produced, thereby ruling out the occurrence of reversible proton transfer. Irreversible deprotonation of 2-butanone by OH⁻ is not unexpected, because the reaction is exothermic by more than 20 kcal/mol,²⁸ and barriers on the potential energy surface, if any, should be small. It is likely that this behavior is general for all anionic bases with proton affinities comparable to that of OH⁻ ($\Delta H_{\text{acid}}(\text{H}_2\text{O}) = 390.7$ kcal/mol).²⁸

Since the enolate ions formed by deprotonation will undergo collisions with their ketone precursors that are present in the flow tube, it is important to determine whether the neutral ketones can act as acid catalysts for isomerizing the initially-formed mixture of tautomeric enolates. It was found that addition of excess ketone to the flow tube resulted in irreversible clustering of the enolate ions with the ketone. However, reaction of the unclustered enolate ions with *n*-butyl nitrite in Q2 gave ratios of surrogate ion intensities that were invariant with changes in the amount of ketone added to the flow tube. This indicates that excess ketone is not able to catalyze enolate ion isomerization, presumably due to the slow rates for the obligatory proton transfer.³¹

The composition of the enolate ions produced upon deprotonation of the three ketones with seven different bases was determined (Table 6). Partial equilibrium cannot be ruled out when these ketones were deprotonated by the conjugate bases of acetonitrile and isobutyronitrile since the acidities of these two molecules are close to that of the ketones (365–370 kcal/mol).²⁸ Also, since fluoride ion deprotonates ketones to yield mixtures of enolates that are close to the equilibrium ratios, it is likely that proton transfer is reversible within the collision complex for this ion-molecule reaction.

Discussion

Methanol-Catalyzed Enolate Tautomerization. The derived rate coefficients for the methanol-catalyzed interconversion of primary and secondary enolates of 2-butanone (Table 2) indicate that this reaction is relatively slow. The average values for k_f and k_r are in the range $5\text{--}6 \times 10^{-11}$ cm³/s, corresponding to reaction efficiencies²¹ ($k_{\text{obsd}}/k_{\text{coll}}$) of about 0.03. Simple clustering of the enolate ions with methanol is the dominant reaction under flowing afterglow conditions, with measured rate coefficients and reaction efficiencies that are larger by a factor of 2. Thus, most of the enolate/methanol collisions are unproductive, *i.e.*, given the total reaction efficiency of about 9%, it follows that about 6 out of every 100 collisions result in cluster formation and 3 out of every 100 lead to enolate isomerization. From these efficiencies it can

be calculated that roughly 200 collisions with methanol molecules are required to convert a pure enolate tautomer to the equilibrium mixture under typical flowing afterglow conditions.³² The inefficiency of the tautomer interconversion arises, in part, from the preferential binding of the methanol catalyst to the oxygen atom of the ambident enolate ion. Shown in Figure 4 is a simplified mechanism for the methanol-catalyzed interconversion of primary and secondary enolate ions by way of a triple-minimum potential energy surface. The 12 kcal/mol difference between the gas-phase acidities of methanol (381 kcal/mol) and 2-butanone (369 kcal/mol) is close to the enolate/methanol binding energy associated with complex A or C (*ca.* 15 kcal/mol).²² As a result, the ketone/methoxide ion complex B that is obligatory for tautomerization lies close in energy to the reactants and products, and its formation from A is relatively unfavorable compared to back-dissociation to reactants.

Enolate Ion Equilibrium Ratios. Previous studies of enolate ions in the gas phase have only partially addressed the issue of the relative thermodynamic stabilities of tautomeric ions. This is due, in part, to the difficulties in determining whether proton transfer occurs reversibly within the initial ion-molecule collision complex, and, if so, whether it is sufficiently rapid to permit complete equilibration of enolate regioisomers on the time scale of the collision. Grützmacher and Sürig have reported that deprotonation of 4,4-dimethyl-2-pentanone-1,1,1-*d*₃ (methyl-*d*₃-neopentylketone) gave the same ratio of (M-D)⁻ to (M-H)⁻ signal intensities when the ketone was deprotonated with either NH₂⁻, F⁻, or OH⁻, thereby suggesting equilibrium control.³³ These investigators also reported that reaction of OH⁻ with 2-hexanone-1,1,1-*d*₃ gave 63% of the primary enolate ion, and reaction with 3-methyl-2-pentanone-1,1,1-*d*₃ gave 97% of the primary enolate ion. These ratios are quite similar to the equilibrium ratios for 2-butanone and 3-methyl-2-butanone, respectively, determined in the present work (Table 3). However, in view of the observation reported in this work that OD⁻ deprotonates 2-butanone irreversibly,³⁰ it is unclear why equilibration of the tautomeric enolate ions would take place in the experiments performed by Grützmacher and Sürig. In another gas-phase study, the competitive loss of H₂ and HD upon CID of deprotonated 2-butanol-3,3-*d*₂ was used to determine the relative stabilities of the primary and secondary enolate ions of 2-butanone.³⁴ After correcting for isotope effects and assuming that deprotonation by hydride occurs under thermodynamic control, the authors concluded that the equilibrium composition consisted of 64% of the secondary enolate ion.

The monitor ion technique has several important advantages over more conventional approaches involving the use of deuterium-labeled ketones for determining the site of deprotonation of an unsymmetrical ketone. For studies of kinetically-controlled deprotonations with deuterated ketones, the primary kinetic isotope effects on the observed (M-H)⁻/(M-D)⁻ ratio would have to be evaluated. Moreover, in equilibrium studies, unavoidable label-scrambling would make the (M-H)⁻/(M-D)⁻ ratio an invalid indicator of the enolate isomer concentrations.

For 2-butanone the equilibrium ratio of primary and secondary enolate ions in the gas phase is close to 1:1, with a slight bias toward the more substituted enolate ion. This outcome is supported by the theoretical results, which indicate essentially equal stabilities for the primary and *Z* secondary isomers. The gas-phase results also compare favorably to what is believed to be the equilibrium ratio of these enolate ions in polar solvents such as dimethylformamide and acetonitrile. For example,

(32) For a total helium pressure of 400 mTorr and flow rate of 200 STP cm³/s, a methanol flow rate greater than 0.7 STP cm³/s is required in order to convert an initial 100:1 mixture of primary and secondary enolates to the 45:55 equilibrium mixture within a reaction distance in the flow tube of 40 cm.

(33) Sürig, T.; Grützmacher, H.-Fr. *Org. Mass Spectrom.* **1989**, *24*, 851.

(34) Haib, J.; Stahl, D. *Int. J. Mass Spectrom. Ion Processes* **1990**, *95*, 289.

(30) Bierbaum, V. M., University of Colorado, personal communication. We are grateful to Dr. Bierbaum for performing this experiment.

(31) Farneth, W. E.; Brauman, J. I. *J. Am. Chem. Soc.* **1976**, *98*, 7891.

Table 4. Calculated Total Energies (Hartrees) and Zero-Point Energies (kcal/mol) for 2-Butanone, 3-Methyl-2-butanone, and Associated Enolate Ions

level	2-butanone	primary enolate	Z secondary enolate	E secondary enolate	3-methyl-2-butanone	primary enolate	tertiary enolate
HF/3-21G	-229.709 35	-229.073 82	-229.073 38	-229.064 58	-268.529 52	-267.898 04	-267.889 65
HF/6-31+G(d)	-231.003 09	-230.388 47	-230.387 07	-230.379 31	-270.036 71	-269.424 64	-269.415 81
MP2/6-31+G(d) ^a	-231.701 66	-231.106 16	-231.105 53	-231.098 01	-270.870 54	-270.278 39	-270.270 61
MP4SDQ/6-31+G(d) ^a	-231.749 30	-231.146 25	-231.145 49	-231.138 19	-270.928 56	-270.328 82	-270.320 81
MP4SDTQ/6-31+G(d) ^a	-231.773 70	-231.174 94	-231.174 28	-231.167 06			
zero-point energy ^b	67.2	59.2	58.8	58.6	84.2	75.9	75.6

^a Geometries optimized at the HF/6-31+G(d) level. ^b Computed from HF/6-31+G(d) frequencies scaled by a factor of 0.89.

Table 5. Calculated Proton Affinities at Carbon and Relative Energies of 2-Butanone and 3-Methyl-2-butanone Enolate Ions

	proton affinity (kcal/mol)	relative energy (kcal/mol)
2-Butanone Enolate ^a		
primary	369.2	0.1
Z secondary	369.1	(0)
E secondary	373.5	4.1
3-Methyl-2-butanone Enolate ^b		
primary	369.5	(0)
	(366.8) ^c	
tertiary	373.8	4.3
	(371.1) ^c	

^a Determined at the MP4SDTQ/6-31+G(d)//HF/6-31+G(d) + ZPE level of theory. ^b Determined at the MP4SDQ/6-31+G(d)//HF/6-31+G(d) + ZPE level of theory. ^c Corrected for estimated effects of including triple excitations in the MP4 energy calculations.

Table 6. Percent Abundance of the Less-Substituted Enolate Ion Obtained by Deprotonation of Ketones by Different Bases

base	proton affinity ^a (kcal/mol)	2-butanone	3-methyl-2-butanone	2-methyl-3-pentanone
NH ₂ ⁻	403.6	58	73	70
HO ⁻	390.8	55	83	74
<i>i</i> -Pr ₂ N ⁻	390.2	58	85	88
tetramethylpiperidide	389.7 ^b	63	85	86
CH ₃ CN ⁻	375.2	38	75	81
(CH ₃) ₂ CCN ⁻	374.6	57	88	84
F ⁻	371.3	45	91	96

^a Taken from ref 28 unless noted otherwise. ^b Reference 42.

treatment of a solution of 2-butanone in acetonitrile with triethylamine and iodotrimethylsilane (generated *in situ*) gave a mixture of primary and secondary trimethylsilyl enol ethers in a ratio of 35:65.³⁵ In another study, Emde *et al.* reported that treatment of 2-butanone with 1 equiv of trimethylsilyl trifluoromethanesulfonate and triethylamine in dichloromethane afforded a 41:59 ratio of primary and secondary trimethylsilyl enol ethers.³⁶ Reaction of 2-butanone with a 20% excess of trimethylsilyl trifluoromethanesulfonate caused this ratio to change to 5:95. Clearly the products are susceptible to isomerization under these reaction conditions. Similarly, House *et al.* have shown that triethylamine hydrochloride is capable of isomerizing alkyl-substituted trimethylsilyl enol ethers.^{3a} These acid-catalyzed isomerizations are representative of the complications that may arise when the "equilibrium ratio" of tautomeric enolate ions is derived by examining the products formed upon trapping of the enolate ions as their trimethylsilyl enol ethers. It is also likely that complete equilibration of the enolate ions was not achieved in some of the above examples.

The arguments offered to explain the slightly greater stability of secondary enolate ions over primary enolate ions are analogous to those used to rationalize the stability ordering of isomeric

alkenes. It is known that internal olefins have lower heats of formation than isomeric terminal olefins. This increase in stability has been attributed to the greater number of favorable hyperconjugative interactions that are available to the more-substituted isomer. Lithium enolates generated in solution under equilibrium conditions tend to yield greater amounts of the more-substituted tautomer than do the corresponding potassium enolates. It has been suggested that the tightly coordinated lithium cation removes electron density from the deprotonated α -carbon more effectively than the potassium cation.³⁷ While hyperconjugation may be partially responsible for these differences, it is difficult to evaluate its role when other effects such as differential solvation of the enolate ions and aggregation effects are operative. Nevertheless, the gas-phase equilibrium results for the 2-butanone enolates obtained in this work indicate that hyperconjugative effects have only a minor influence, if any, on enolate stability.

The stability ordering is reversed for the 3-methyl-2-butanone and 2-methyl-3-pentanone enolates when compared to the 2-butanone tautomers. The present measurements indicate that for both isopropyl-substituted ketones there is a strong preference for formation of the *less* substituted enolate ion under equilibrium conditions. The 98:2 and 95:5 equilibrium ratios measured for these two systems indicate that the tertiary enolate ions are destabilized relative to their primary and secondary isomers by 2.3–1.7 kcal/mol. The *ab initio* calculations for the 3-methyl-2-butanone enolates suggest an even greater energy difference. Combining the 4.3 kcal/mol computed enthalpy difference between the enolate tautomers with the calculated difference in absolute entropies (3.2 eu) gives a free energy difference at 298 K of 3.3 kcal/mol. The decreased stability of the tertiary enolate ions can be understood in terms of two competing effects. On the one hand, α -methyl substitution is expected to have a small stabilizing influence on the enolate ion, as in the case of the secondary enolate of 2-butanone. On the other hand, the increase in A_{1,3} (allylic) strain³⁸ is expected to destabilize the enolate ions of α -dialkyl-substituted acyclic ketones. For comparison, the heat of formation of *cis*-2-butene is 1.0 kcal/mol higher than that of *trans*-2-butene.³⁹



This value can be used as an approximate indicator of the strain in the enolate ion that results from two methyl groups in a *cis* arrangement. This steric effect will dominate the weak stabilizing influence of the methyl groups in the enolate. The theoretical

(35) Cazeau, P.; Duboudin, F.; Moulines, F.; Babot, O.; Dunogues, J. *Tetrahedron* 1987, 43, 2075.

(36) Emde, H.; Götz, A.; Hofmann, K.; Simchen, G. *Liebigs Ann. Chem.* 1981, 1643.

(37) (a) House, H. O.; Trost, B. M. *J. Org. Chem.* 1965, 30, 1341. (b) House, H. O.; Auerbach, R. A.; Gall, M.; Peet, N. P. *J. Org. Chem.* 1973, 38, 514. (c) House, H. O.; Prabhu, A. V.; Phillips, W. V. *J. Org. Chem.* 1976, 41, 1209.

(38) (a) Johnson, F. *Chem. Rev.* 1968, 68, 375. (b) Hoffmann, R. W. *Chem. Rev.* 1989, 89, 1841.

(39) Pedley, J. B.; Naylor, R. D.; Kirby, S. P. *Thermochemical Data of Organic Compounds*, 2nd ed.; Chapman and Hall: London, 1986.

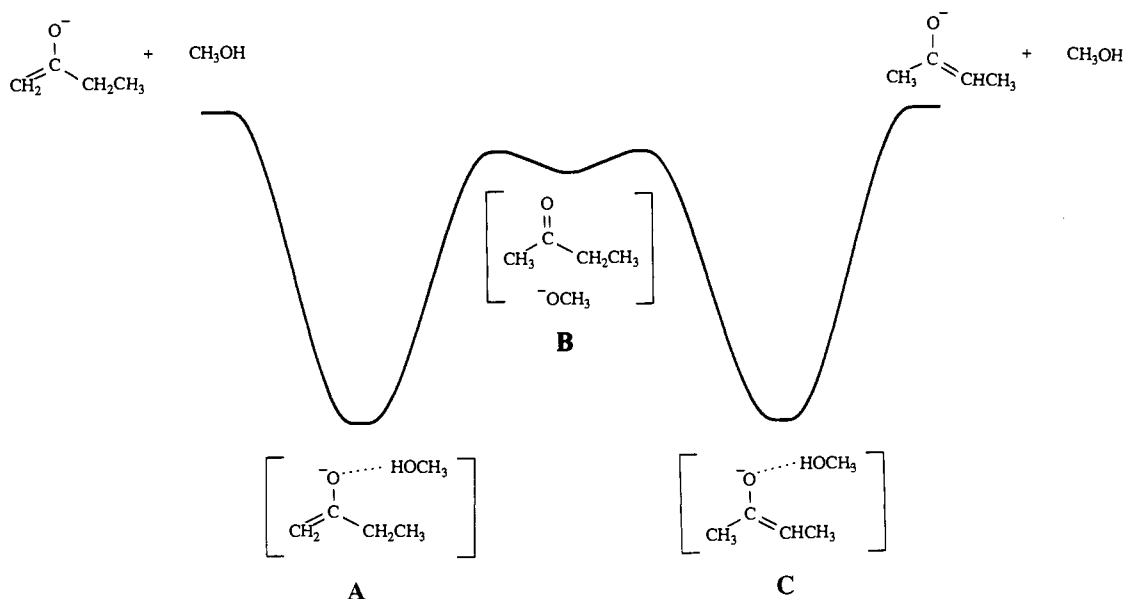
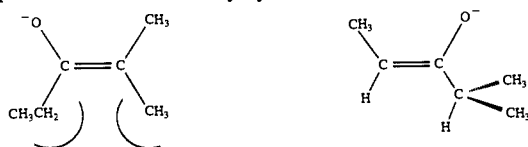


Figure 4. Schematic reaction-energy profile for methanol-catalyzed tautomerization of primary and secondary enolate ions of 2-butanone.

results are consistent with this view, in that the tertiary enolate of 3-methyl-2-butanone and the *E* secondary enolate of 2-butanone are destabilized with respect to the corresponding primary enolate ions by the same amount.

It is important to note that the equilibrium results reported here for 3-methyl-2-butanone and 2-methyl-3-pentanone enolates are not unique to the gas phase. Brown has shown that the equilibrium mixture of potassium enolates of 3-methyl-2-butanone prepared in tetrahydrofuran at room temperature comprises 88% of the less substituted isomer.⁴⁰ Similarly, House and Trost found that equilibration of the lithium enolates of 2-methyl-3-pentanone with excess ketone results in greater than 98% of the less-substituted enolate ions.^{37a} Additional evidence for destabilization of acyclic tertiary enolate ions due to steric effects is demonstrated in the carbon acidities of acetophenone, propiophenone, and isobutyrophenone measured in dimethyl sulfoxide. Bordwell and co-workers found that the pK_a of propiophenone is slightly lower than that of acetophenone, while the pK_a of isobutyrophenone is higher than both compounds.⁴¹ These investigators proposed that the apparent stability ordering is due to steric inhibition to solvation by the methyl group in isobutyrophenone. The gas-phase results reported here suggest that differential solvation may not be the reason, but rather it is an intrinsic effect in the enolate, such as the allylic strain between the methyl group and the phenyl group.

The enolate ions of 2-methylcyclohexanone are frequently used as examples in discussions of enolate ion stability.^{2,3} For this ketone, formation of the more substituted enolate ion is favored under equilibrium conditions, thus illustrating the importance of alkyl substitution. However, this example is somewhat misleading since both the secondary and tertiary enolate ions of 2-methylcyclohexanone possess approximately equal $A_{1,3}$ steric interactions. As a result, the stabilizing effect of the methyl group controls the stability ordering for the enolate ions of 2-methylcyclohexanone. The secondary enolate ion of 2-methyl-3-pentanone is able to avoid the unfavorable allylic interaction *via* the *Z* diastereomer, while the tertiary enolate ion cannot. Thus, the stability ordering for these two enolate ions is inverted when compared to the enolate ions produced from 2-methylcyclohexanone.



Effect of the Base on the Kinetic Deprotonation of Ketones. The results shown in Table 6 indicate that amide deprotonates

the three ketones used in this study in a statistical fashion, *i.e.*, the observed isomer ratios are determined by the relative number of hydrogens present at the α and α' positions of the ketone. As the strength of the base decreases, there is an increase in the selectivity of the deprotonation toward the more stable enolate ion. The bases OH^- , *i*- Pr_2N^- , and tetramethylpiperidide provide a good test of steric effects on the deprotonation of ketones in the gas phase because, even though these bases have widely varying structures, their proton affinities are all within 1 kcal/mol of each other.⁴² The experimental results indicate that as the steric bulk of the base is increased, there is only a slight increase in the yield of the less substituted enolate ion.

The reactivity of *i*- Pr_2N^- and tetramethylpiperidide toward ketones in the gas phase differs markedly from what is observed for lithium dialkylamide bases in the condensed phase. Saunders and co-workers have shown that the less-substituted enolate ion comprises 89% of the enolate ions when 2-pentanone is deprotonated with lithium diisopropylamide (LDA) in tetrahydrofuran at 0 °C.^{43a} Under similar conditions, 3-methyl-2-butanone and 2-methyl-3-pentanone generate the less-substituted enolate ions in 99% and 91% fractional abundances, respectively.^{43b} Assuming that 2-pentanone is a suitable model for 2-butanone, the selectivities of LDA in solution substantially exceed the selectivity of *i*- Pr_2N^- toward these ketones in the gas phase. At the very least, this comparison confirms the importance of the counterion in the regioselective deprotonation of ketones by LDA and related bases in solution.

The exact nature of LDA and lithium tetramethylpiperidide in solution is still unresolved, and numerous experimental observations demonstrate that the deprotonation of ketones with these bases is a complex process. Saunders and co-workers used kinetic isotope studies to show that LDA exists as more than one active base in solvents such as tetrahydrofuran and 1,2-dimethoxyethane.⁴³ Addition of hexamethylphosphoric triamide (HMPA) to the LDA solution gives rise to kinetic isotope effects that are consistent with a single species that deprotonates the ketone. Clearly, the degree of aggregation of the base is an important consideration in evaluating the selectivity of LDA in

(40) Brown, C. A. *J. Org. Chem.* **1974**, *39*, 1324.

(41) (a) Bordwell, F. G.; Harrelson, J. A., Jr. *Can. J. Chem.* **1990**, *68*, 1714. (b) Bordwell, F. G.; Branca, J. C.; Johnson, C. R.; Vanier, N. R. *J. Org. Chem.* **1980**, *45*, 3884. (c) Bordwell, F. G.; Bartmess, J. E.; Hautala, J. A. *J. Org. Chem.* **1978**, *43*, 3095.

(42) Grimm, D. T.; Bartmess, J. T. *J. Am. Chem. Soc.* **1992**, *114*, 1227.

(43) (a) Xie, L.; Saunders, W. H., Jr. *Z. Naturforsch.* **1989**, *44a*, 413. (b) Beutelman, H. P.; Xie, L.; Saunders, W. H., Jr. *J. Org. Chem.* **1989**, *54*, 1703. (c) Xie, L.; Saunders, W. H., Jr. *J. Am. Chem. Soc.* **1991**, *113*, 3123.

solution. In studies aimed primarily at addressing the *E* vs *Z* selectivity in the deprotonation of ketones, Collum and co-workers have shown that the identity of the active base will change during the course of the reaction.⁴⁴ This effect causes the ratio of diastereomeric enolate ions to vary as a function of the extent of the reaction.

The results obtained for the irreversible deprotonation of 2-butanone, 3-methyl-2-butanone, and 2-methyl-3-pentanone in the gas phase with various anionic bases underscores the important influence of extrinsic factors on the formation of enolate ions from ketones in solution. The original studies by Ireland and co-workers⁴⁵ recognized some of the features that determine the relative stabilities of the transition states for the competing deprotonation reactions. The results of the present study strongly suggest that the solvent, counterion, and associated aggregates are indispensable elements in regioselective deprotonation of unsymmetrical ketones. Without them, essentially indiscriminate deprotonation will take place.

Conclusions

For the three unsymmetrical ketones examined in this study, the thermodynamic stabilities of the tautomeric pairs of enolate ions generated in the gas phase follow the same basic trend as has been observed in solution. The intrinsic stability ordering of acyclic, aliphatic ketone enolate ions is $2^\circ \geq 1^\circ \gg 3^\circ$. α -Methyl substitution has a small but measurable stabilizing influence on

(44) (a) Galiano-Roth, A. S.; Kim, Y.-J.; Gilchrist, J. H.; Harrison, A. T.; Fuller, D. J.; Collum, D. B. *J. Am. Chem. Soc.* **1991**, *113*, 5053. (b) Hall, P. L.; Gilchrist, J. H.; Collum, D. B. *J. Am. Chem. Soc.* **1991**, *113*, 9571. (c) Hall, P. L.; Gilchrist, J. H.; Harrison, A. T.; Fuller, D. J.; Collum, D. B. *J. Am. Chem. Soc.* **1991**, *113*, 9575.

(45) (a) Ireland, R. E.; Willard, A. K. *Tetrahedron Lett.* **1975**, 3975. (b) Ireland, R. E.; Mueller, R. H.; Willard, A. K. *J. Am. Chem. Soc.* **1976**, *98*, 2868.

the enolate ion in the absence of $A_{1,3}$ steric interactions. The tertiary enolate ions of 3-methyl-2-butanone and 2-methyl-3-pentanone are destabilized by the $A_{1,3}$ strain between the *cis* methyl groups. This unfavorable interaction dominates any hyperconjugative stability that is gained by forming the more substituted enolate ion.

Since statistical ratios of enolate ions are produced when ketones are deprotonated by strong and hindered bases in the gas phase, the term "kinetic control" is probably a misnomer when describing the analogous reactions in solution. The relative unselectivity of bases such as diisopropylamide and tetramethylpiperidide in the gas-phase deprotonation of ketones attests to the importance of the Ireland model and variations thereof to explain the high regioselectivity of these reactions in solution.

The experimental methods developed in this study for identifying and quantitating regioisomeric enolate ions cannot distinguish the *E* and *Z* diastereomers that could be produced from acyclic ketones. We are currently developing an alternate procedure for quantitative analysis of *Z/E* mixtures of enolates formed by gas-phase ion-molecule reactions.

Acknowledgment. We are indebted to the National Science Foundation (CHE-9221480) for generous financial support for this work.

Supplementary Material Available: Optimized geometries in GAUSSIAN 92 z-matrix format and harmonic vibrational frequencies obtained at the HF/6-3+G(d) level are available for 2-butanone, 3-methyl-2-butanone, and each of the corresponding enolate ions (5 pages). This material is contained in many libraries on microfiche, immediately follows this article in the microfilm version of the journal, and can be ordered from the ACS; see any current masthead page for ordering information.